

INFLUENCE OF METAKAOLIN ON RESISTIVITY OF CEMENT MORTAR TO MAGNESIUM CHLORIDE SOLUTION

HISHAM M. KHATER

*Housing and Building National Research Centre (HBNRC)
87 El-Tahreer St., Dokki, Giza, P.O. Box 1770 Cairo, Egypt*

E-mail: Hkhater4@yahoo.com

Submitted April 23, 2010; accepted October 17, 2010

Keywords: Cement, Pozzolana, Mortar, Magnesium chloride

An experimental study for the resistance of mortar specimens incorporating 0%, 5%, 10%, 15%, 20%, 25% and 30% metakaolin [produced by firing Kaolin at 820 °C for 2 hrs (MK)] to the magnesium chloride solution was reported. Results confirmed that mortar specimens with a high replacement level of metakaolin showed higher resistance to magnesium solution. Due to, the reduction of calcium hydroxide and the increase of secondary C–S–H in the cement matrix due to pozzolanic reaction of metakaolin. Compressive strength values of the blended OPC mortars specimens were improved relative to those contains no MK up to 25 wt.% OPC substitution, and the following decrease up to 30 wt.% MK. SEM microstructures indicate a good improvement for the matrix structure of the blended cement mortars where a more dense structure was observed.

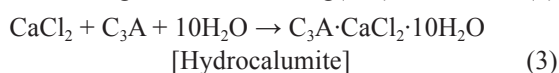
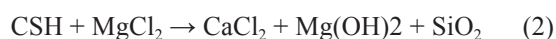
INTRODUCTION

In recent years, metakaolin (MK) was studied because of its high pozzolanic properties [1-2]. It is well known that MK is a reactive aluminosilicate, which is formed by the dehydroxylation of kaolin precursor upon heating in the temperature range of 700–800°C [3-4]. The effects of MK on the durability and mechanical properties of mortar or concrete have been widely reported [5-7]. The performance of concrete incorporating MK, at appropriate replacement levels, is similar to that of concrete containing silica fume. Recent works have shown that MK is effective as a supplementary cementitious material on improving the durability of concrete, for example, alkali–silica reaction [9] and resistance to chloride ingress [9].

The influence of chloride is either chemical by interaction with liberated lime from the hydration reaction forming what is known as Friedel's salt or hydrocalumite ($C_3A \cdot CaCl_2 \cdot 10H_2O$) causing softening to the composition as indicated from the following equations:



and



While the other most dangerous role is the free chloride ions that cause corrosion for the reinforcement steel in concrete leaving it damaged. Metakaolin (MK) recently has been added to the list of pozzolanic materials [10], as it is silica based products that, on reaction with CH, produces C–S–H gel at ambient temperature so that prevent free lime from reaction with tricalcium aluminates forming hydrocalumite as represented by the latter equation. MK also contains alumina that, on reaction with CH, produces additional alumina containing phases, including C_4AH_{13} , C_2ASH_8 , and C_3AH_6 [11].

The present article reports our findings of the effects of MK on resistance to magnesium chloride attack as indicated from phase formation and some of the resulting physical and microstructural properties when MK is introduced as a cement replacement in OPC-Mk cement mortar specimens; followed by water curing up to 28 days (zero time) followed by immersion in magnesium chloride solution (5 %) up to 360 days.

EXPERIMENTAL

Starting materials

The materials used in this investigation are ordinary Portland cement (OPC) obtained from Suez Cement Company (Tourah plant), Egypt. Kaolin with

high kaolinite content, provided from Al Dehesa, Sinai governorate, Egypt, was thermally treated at 820°C for 2 hrs with a heating rate of 5°C/min, to produce metakaolin (MK). This temperature was chosen on the basis of an earlier research work [12]. The most important characteristics of this calcined product (MK) are: chemical composition ($\text{SiO}_2 + \text{Al}_2\text{O}_3$ about 95 %), fineness (surface area between 15 and 20m²/g), and its poorly crystalline nature. The results of chemical analyses of the starting materials are shown in Table 1. The calcinations below 700°C results in a less reactive metakaolinite with more residual kaolinite, above 850°C crystallization occurs and reactivity declines [13].

Preparation of mortar mixes

Six different blended cement mortar mixtures were prepared. OPC was partially substituted with 0 %, 10 %, 15 %, 20 %, 25 % and 30 % of MK by mass. The water-binder material ratio (w/b) was 0.60 by mass. The cementitious material/fine sand (<1.0 mm) was in the ratio of (1:3) in all mortar mixtures. All mortar specimens were mixed in a standard planetary mixer for 5 min continuously, and then poured in 2.5 × 2.5 cm steel moulds, left at 100 % relative humidity for 24 hours, demoulded and water cured up to 28 days (as zero time) in tape water after then removed from the tape water container and immersed in magnesium chloride solution (5 %) for one year [i.e., 13 g/l of Mg^{2+} and 19 g/l of Cl^-]. The solution was renewed every month to keep the concentration as much as possible constant. After curing, the cubes were then dried well at 80°C for 24 hr at each age and then the cubes were exposed to the compressive strength measurements and then subjected to stopping of the hydration process using stopping solution to prevent further hydration and for further analysis.

Methods of investigation

Chemical analysis was carried out using XRF Spectrometer PW1400. The removal of free water was accomplished by using alcohol/acetone method as recommended by different investigators [14]. Compressive strength tests were carried out using five tones German Brüt pressing machine with a loading rate of 100 kg/min determined according to the ASTM [15]. The XRD analysis was carried out using a Philips PW 1050/70 Diffractometer. The data were identified according to the XRD software (pdf-2: database on CD-Release 2005). The DTA was followed using a DT-50 Thermal Analyzer (Schimadzu Co-Kyoto, Japan).

The data were compared with DTA standard data [16]. Some physico-mechanical properties, e.g. bulk density, water absorption, and compressive strength were determined according to the Egyptian Standards [18]. The microstructure of the hardened blended cement mortars was studied using SEM Inspect S (FEI Company, Holland) equipped with an energy dispersive X-ray analyzer (EDX).

Table 1. Chemical composition of starting materials (wt.%).

| Oxide | OPC | Kaolin | MK |
|--------------------------|-------|--------|-------|
| SiO_2 | 21.20 | 44.64 | 52.26 |
| Al_2O_3 | 5.22 | 38.9 | 42.93 |
| Fe_2O_3 | 3.24 | 0.95 | 1.01 |
| CaO | 62.66 | 0.55 | 0.43 |
| MgO | 1.78 | 0.25 | 0.26 |
| Na_2O | 0.41 | 0.31 | 0.02 |
| K_2O | 0.19 | 0.01 | 0.19 |
| SO_3 | 3.07 | 0.22 | 0.52 |
| TiO_2 | 0.11 | 1.64 | 1.87 |
| P_2O_5 | 0.09 | 0.07 | 0.01 |
| L.O.I. | 1.94 | 12.01 | 0.39 |
| Total | 99.71 | 99.55 | 99.89 |
| Cl^- | 0.04 | - | - |
| $\text{Na}_2\text{OEq.}$ | 0.54 | - | - |
| L.S.F | 0.89 | - | - |
| C_3A | 8.36 | - | - |
| C_3S | 45.45 | - | - |
| C_2S | 26.58 | - | - |
| C_4AF | 9.85 | - | - |

RESULTS AND DISCUSSION

Phase composition

The XRD patterns of one day (after 28days in water)-magnesium chloride cured neat blended cement mortar specimens at different curing ages in 5 % magnesium chloride solution are shown in Figure 1. The patterns show that, the presence of Quartz (SiO_2), portlandite $\text{Ca}(\text{OH})_2$, Unhydrated cement particles [Iarnite ($\beta\text{-C}_2\text{S}$) as well as C_3S], Gehlenite hydrate (C_2ASH_8), Calcite(C), CSH, Brucite (B) and Friedel's salt (FS) which are the expected products formed by cement mortar hydration and magnesium chloride attack. The patterns show that, the intensity of the main portlandite ray $\text{Ca}(\text{OH})_2$ (18.18 and 34.08 2 θ) decreases with curing time up 360 days, as it is consumed in the reaction with the active metakaolin forming additional CSH phases. Quartz (SiO_2) is almost constant up to 360 days. Unhydrated cement particles [Iarnite ($\beta\text{-C}_2\text{S}$) as well as C_3S] decreases up to 360 days due to the progress of hydration reaction. Another observation is the a great amount of Friedel's salt (11.39, 22.78, 31.17 and 38.99 2 θ) at 90 days, then increases with time up to 360 days.

Also, brucite was detected from its small peaks (18.5° and 38.0° 2 θ) as a result of interaction of magnesium chloride with liberated lime. CSH contents increase as curing age goes on up to 360 days which reflect the progress of hydration reaction.

The XRD patterns of 270 days magnesium chloride cured specimens containing various content of metakaolin are shown in Figure 2. The patterns show that, gehlenite hydrate (C_2ASH_8) appears as the predominant phase of the pozzolanic reaction between MK and calcium

hydroxide, increasing with MK addition up to 30 %, but due to its low crystallinity; it does not appear in the XRD patterns unless MK content beyond 30 %, whereas it precipitates when replaces OPC [13]. Beyond 90 days of curing, the lime is totally consumed by pozzolanic reaction; fact will be in agreement with a prior study [19] which reported that metakaolin reacts with 1.2 times its mass of portlandite. Whilst the produced portlandite is consumed completely due to its reaction with the active metakaolin which have very fine pores of size $<0.3\mu\text{m}$ leading to more compaction and densifying of the mortar structure.

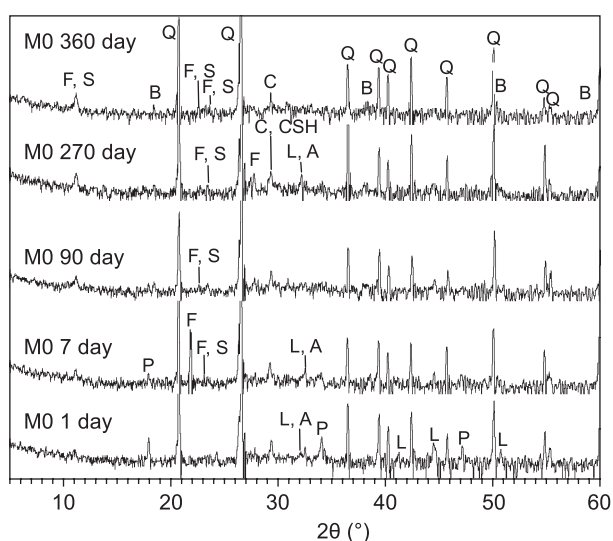


Figure 1. XRD patterns of one up to 360 days magnesium chloride cured specimens ($w/b = 0.60$) without Mk; A - C_3S , L - $\beta-C_2S$, P - $Ca(OH)_2$, C - $CaCO_3$, CSH - Calcium silicate hydrate, GH - C_2ASH_8 , B - $Mg(OH)_2$, F - Feldspars, FS - Friedel's salt.

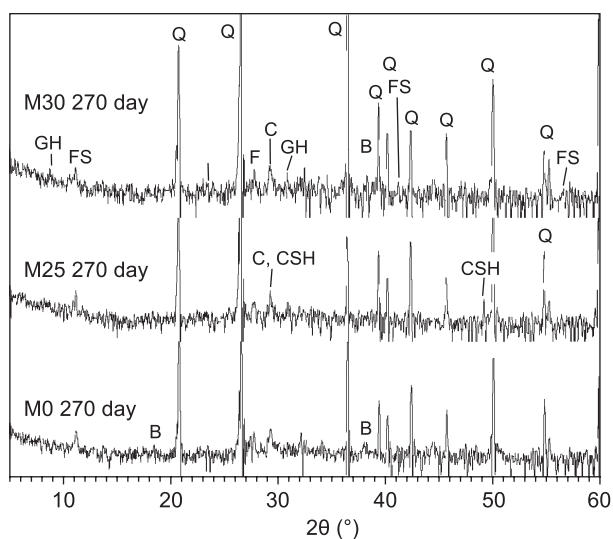


Figure 2. XRD patterns of 270 day magnesium chloride cured specimens ($w/b=0.60$) with different content of added Mk; A - C_3S , L - $\beta-C_2S$, P - $Ca(OH)_2$, C - $CaCO_3$, CSH - Calcium silicate hydrate, GH - C_2ASH_8 , B - $Mg(OH)_2$, F - Feldspars, FS - Friedel's salt.

Calcite content increases with curing time while CSH phases increases up to maximum at 25 % MK content, then they decrease at 30 % where the metakaolin acts only as filler due to the dilution effect of cement component. Whilst the quartz content is almost constant with increase of MK content. Friedel's salt decreases in its intensity with MK addition up to 25 %, then it becomes predominant at 30 % MK as the dilution effect of MK making mortar structure more susceptible to magnesium chloride attack. A noticeable brucite peaks appears at 0 % MK then decreases at 25 % MK, while at 30 % MK the higher MK content facilitate the formation of brucite as it acts as a filler leaving the structure porous, so that will able to incorporate more brucite that is an insoluble material, lower alkalinity of hydration materials leading to destabilization of the hydration materials and hence deterioration.

XRD patterns of 360 days magnesium chloride cured specimens containing various content of metakaolin are shown in Figure 3. The patterns show the increase of the amount gehlenite hydrates (C_2ASH_8) with the increase of MK contents. In the case of blended cements containing lower than 25 % MK, the XRD patterns shows traces of C_2ASH_8 phase (weak peak at $2\theta = 7.2^\circ$). This fact means the very low crystallinity of C_2ASH_8 phase in blended cements. These findings totally agree with prior results [13], only detected the presence of C_2ASH_8 in blended cement with MK contents of 30% or more at 360 days of curing time. Also, it can be noticed the increase of CSH with curing time as the hydration reaction is in progress and then transformed to its crystalline tobermorite form. Brucite decreases sharply with MK addition as well as with time which may be due to its recrystallization to its hydrated magnesium chloride form and leached on

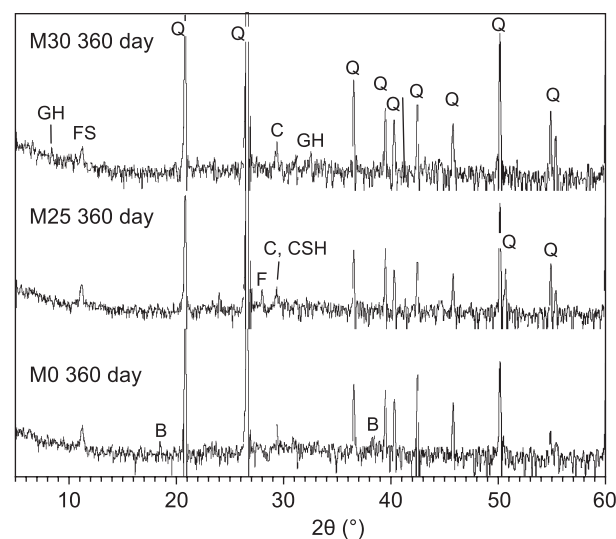


Figure 3. XRD patterns of 360 days magnesium chloride cured specimens ($w/b = 0.60$) with different content of added MK; A - C_3S , L - $\beta-C_2S$, P - $Ca(OH)_2$, C - $CaCO_3$, CSH - Calcium silicate hydrate, GH - C_2ASH_8 , B - $Mg(OH)_2$, F - Feldspars, FS - Friedel's salt.

the surface or participate in the mortar expansion, which accompanied by stabilization in Friedel's salt (FS) content.

The DTA curves of neat metakaolin specimens that cured in magnesium solution from one and 360 days are shown in Figure 4. The patterns show, the presence of endotherms below 200°C for free water, CSH (I) and tobermorite gel, endotherms at about 299 - 302°C for well crystallized tobermorite, at 373 - 382°C for Friedel's salt, endotherms at about 462°C for dehydroxylation of portlandite and endotherms at about 580-585°C for ($\alpha \rightarrow \beta$) quartz conversion as well as endotherms at about 683-693°C for decarbonation of ill-crystalline calcite. While, the exotherms at about 894-922°C for calcium and silica interaction or wollastonite.

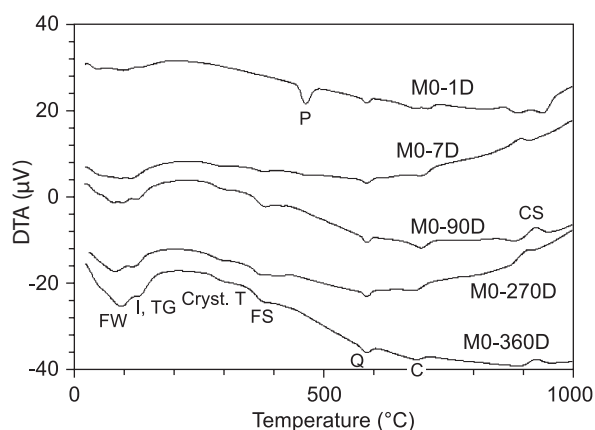


Figure 4. DTA curves of one up to 360 days-magnesium chloride cured ($w/b = 0.60$) specimens; FW - Free water, P - Portlandite, C - ill-crystalline calcite, Q - Quartz, I - CSH(I), TG - Tobermorite gel, GH - C_2ASH_8 , Cryst. T - Well crystalline tobermorite, FS - Friedel's salt, CS - Wollastonite.

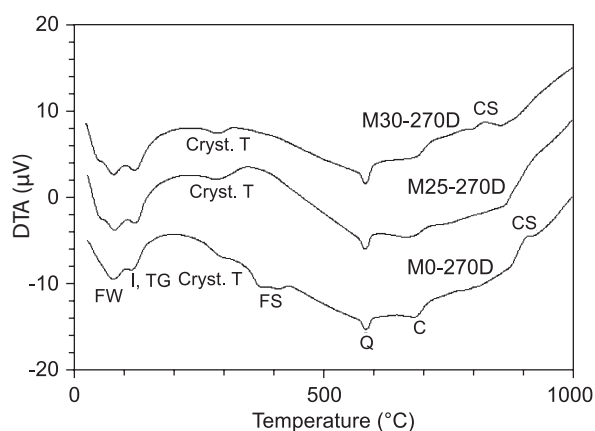


Figure 5. DTA curves of 270 days magnesium chloride cured ($w/b = 0.60$) specimens with variant MK content; FW - Free water, P - Portlandite, C - ill-crystalline calcite, Q - Quartz, I - CSH(I), TG - Tobermorite gel, GH - C_2ASH_8 , Cryst. T - Well crystalline tobermorite, FS - Friedel's salt, CS - Wollastonite.

The endothermic peaks of CSH (I) and tobermorite gel increases with curing time up to 360 days as the hydration reactions proceed which accompanied by a decrease of portlandite up to complete vanishing at 7 days and a noticeable appearance of Friedel's salt beyond 90 days and slightly increase up to 360 days as it consumes the liberated lime from the hydration reaction. Quartz is almost unchanged with curing time while calcite peak is nearly small up to 360 days as all lime was incorporated in interaction with magnesium solution and tricalcium aluminates forming Friedel's salt. A noticeable increase of exothermic peak of CS indicating the increase of CSH (I) and also its high degree of crystallinity up to 360 days.

The DTA curves of 270 and 360 days cured specimens with variable metakaolin content are shown in Figures 5 and 6. The patterns indicate the growth of hydration phases as represented by CSH (I) and tobermorite gel both reach the maximum at 25 % MK then decreases up to 30 % MK but they are not proportional to OPC content due to the effectiveness of the pozzolanic reaction. On the other hand, Friedel's salt exhibit a marked decrease with Mk addition which emphasized also by the XRD patterns Figures 2 and 3. Calcite content slightly increases with curing time.

Scanning electron microscopy (SEM)

The microstructure and the morphology of the hardened OPC-MK mortar specimens containing no metakaolin content immersed in 5 % $MgCl_2$ (water cured up to 28 days) at 1, 7, 90 days are shown in Figure 7. The scanning electron micrographs (SEM) of the neat OPC mortar specimens after one day of hydration Figure 7a, showed the spreading of the hydration products all over the surface as well as the presence of massive layer of calcium hydroxide that covered also with the hydration materials that was confirmed latter by XRD

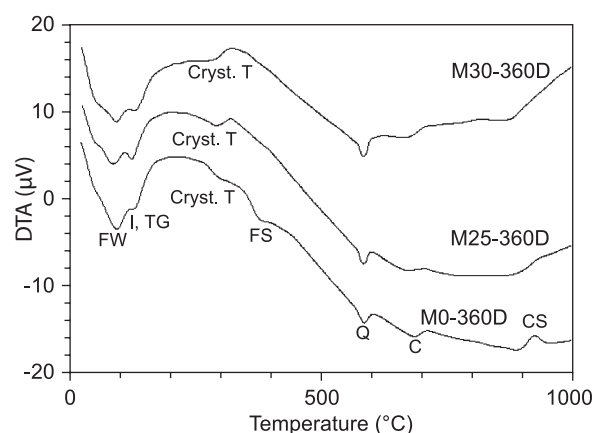
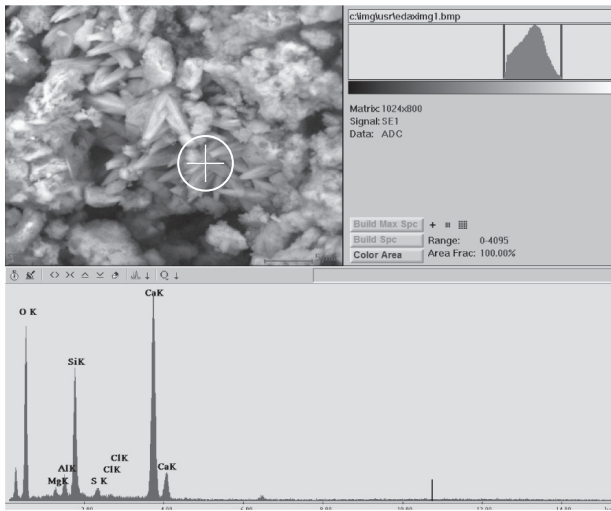


Figure 6. DTA curves of 360 days magnesium chloride cured ($w/b = 0.60$) specimens with variant MK content; FW - Free water, P - Portlandite, C - ill-crystalline calcite, Q - Quartz, I - CSH(I), TG - Tobermorite gel, GH - C_2ASH_8 , Cryst. T - Well crystalline tobermorite, FS - Friedel's salt, CS - Wollastonite.

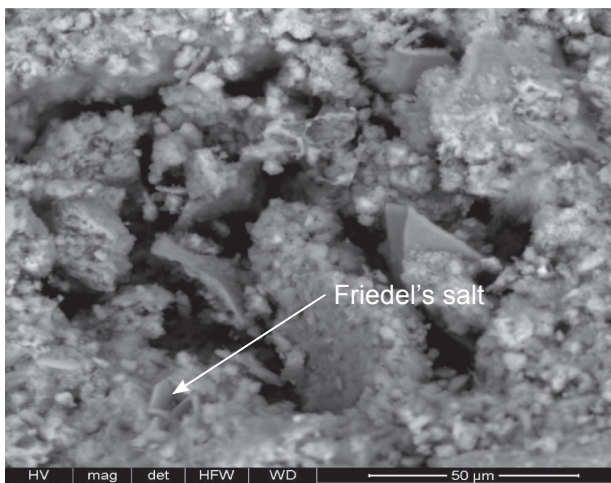


having a sharp portlandite peak at that age. The EDX analysis confirms the presence of honeycomb CSH (II) that contains high calcium content than the silica. After 7 days, the micrograph indicates the growth of hydration products with the increase of ill-crystallized CSH phases and hexagonal crystals of $\text{Ca}(\text{OH})_2$ as well as little plates of Friedel's salt that appear within the matrix Figure 7b.

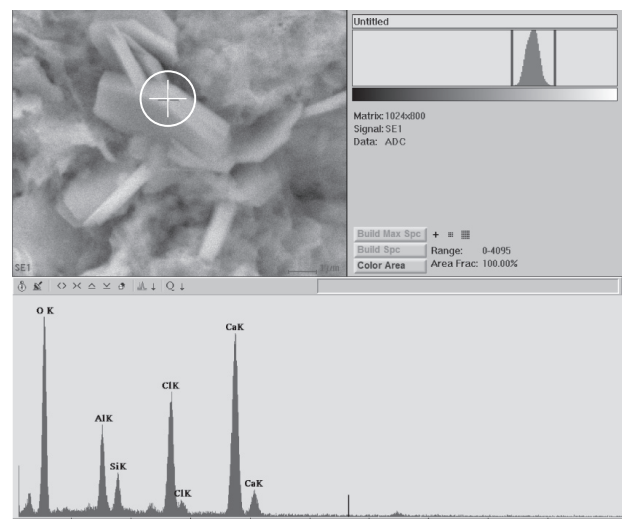
Whilst at 90 days, the hydration went steadily whereas the most obvious note is the presence of ill-crystalline FS, demonstrated from the EDX analysis, overlapping with most of the hydration products and filling the pores resulting in a more compaction at these ages. Where, the attack of magnesium chloride producing brucite ($\text{Mg}(\text{OH})_2$), which has low solubility, assumed to envelop the remainder of the cement gel and protect it against further deterioration [17]. After 360 days, the microstructure seems different where a noticeable pore is filled with FS (thin hexagonal crystals) that appears to be crystalline in nature (Figure 8a). The EDX analysis



a)

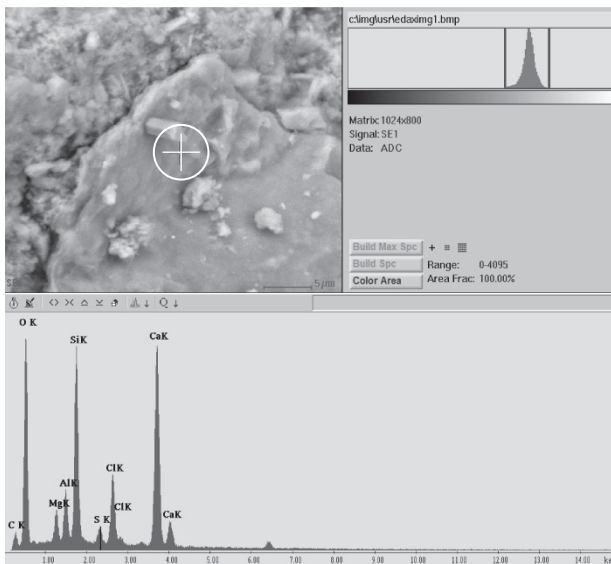


b)



c)

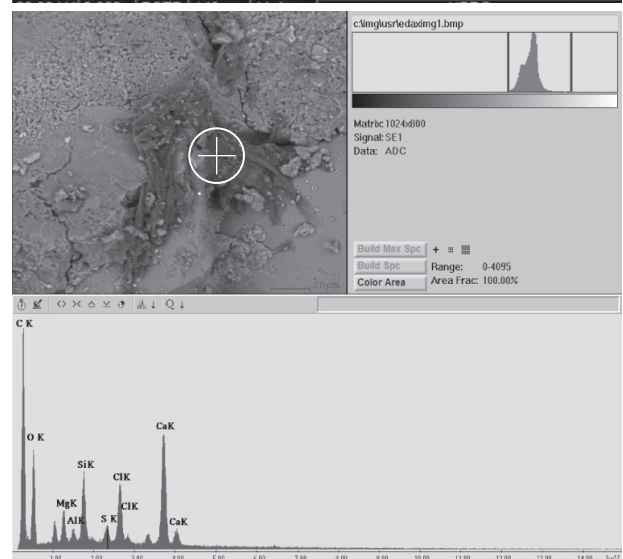
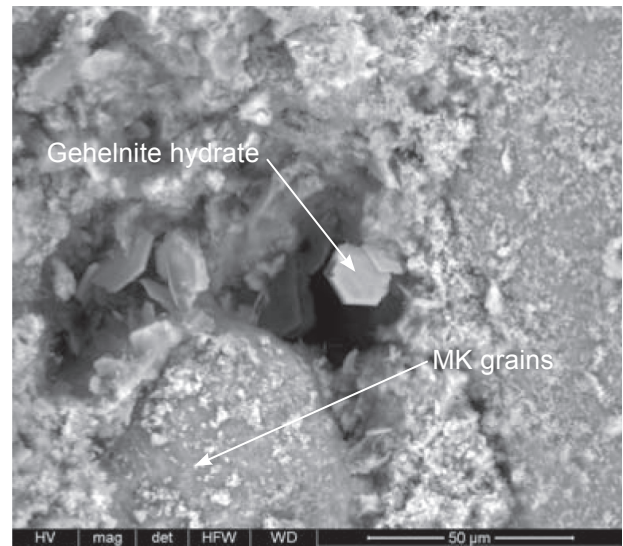
Figure 7. SEM micrograph of the neat OPC blended cement mortar specimens without metakaolin addition at W/C=0.60, magnesium chloride at (a) one day, (b) 7 days and (c) 90 days.



a)

for this age also indicate the presence of Ca, Si, Al and Cl where it's possible that those values of EDX incorporate calcium and silicon from hydrated cement matrix (Figure 8a). Also, Cl ions seem to be fused within the hydration materials leading to an enhancement in the physico-mechanical properties.

With an increased substitution of OPC by Mk up to 25 wt.% and immersed in $MgCl_2$ solution up to 360 days Figure 8b, the SEM micrograph indicated a relatively dense and compact structure where the cement binder exhibited a relatively low porosity. The content of CSH gel phases increases with the co-existence of the two types of CSH phases; these are CSH (II) which has a platy (honeycomb) type structure and CSH(I) with its fiber-like structure. Also, we can notice the presence of well crystalline CSH all over the matrix structure and fibrous one within the pores with slight crystals of gehlenite hydrate.



c)



b)

Figure 8. SEM micrograph of the neat OPC blended cement mortar specimens without metakaolin addition at W/C = 0.60, magnesium chloride at 360 days (a) 0 % MK (b) 25 % MK and (c) 30 % MK.

The SEM micrographs of the hardened OPC-Mk blended cement mortar specimens having 30 % M and immersed in magnesium solution up 360 days are represented in Figure 8c. The micrograph consisted primarily of poorly crystalline structure as the cement content was decreased sharply producing low content of hydrated lime compared with the last mentioned structure of 25 % MK. Whilst, the gehlenite hydrates become a predominant as Mk is in excess also higher content of metakaolin grains dispersed on the matrix surface acting mainly as a filler.

Physico-mechanical properties

Compressive strength

The results of compressive strength as a function of metakaolin content and curing time up to 360 days are shown in Table 2 and represented in Figure 9. The results show the increase of compressive strength at any metakaolin addition with curing time, exceeding that of the reference mortar specimens at all curing time as result of binder formation and accumulation in the open pores caused by cement hydration as well as the pozzolanic reaction of metakaolin with CH

The rate of strength development in PC is mainly dependent on the hydration rate of clinker, while in PC-MK systems it is dependent on the combination of PC hydration and the pozzolanic activity of metakaolin. According to the literatures, the main factors that affect the contribution of metakaolin in strength are: (a) the filler effect, (b) the dilution effect (physical effect) and (c) the pozzolanic reaction of metakaolin with CH (chemical effect) forming additional CSH phases according to [21].

From 0 up to 25 % replacement of PC with MK, the increase of relative strength is mainly attributed to the filler effect leading to an initial acceleration of PC hydration and the increase of CSH binder phases caused by the reaction of CH liberated from cement hydration and metakaolin's SiO₂ component, while the decrease of the relative strength beyond 25 %, may be due to the cessation of the pozzolanic reaction and the filler effect is surpassed by the dilution effect leading to low of the relative strength than that observed at 25 % metakaolin or overcoming the filling effect over the pozzolanic one as the source of liberated lime (PC) decreases.

From the XRD data Figure 1, cement phases decrease while CSH increases with the increase of curing time up to 360 days which explain the strength increase, also emphasized by DTA analysis that show the increase of CSH(I), tobermorite gel and crystalline tobermorite up to 360 days. While, with MK content the increase of strength up to 25 % is explained by the higher content of CSH and crystalline tobermorite while at 30 % MK, the gehlenite hydrate appears which has low pozzolanic properties as explained from Figures 2-6 where, according to [22], the best correlation exists

between the total sum of tobermorite and C-S-H present and the compressive strength. Also, FS that formed at later ages of hydration exhibit an increase in its intensity in neat mixes with a slight increase in brucite content up to 360 days and also decrease with MK up to 25 % due to the incorporation of liberated lime in the formation of hydrating materials with MK, while at higher ratio from MK (beyond 30 %) the FS increases as the dilution effect of MK overcome the pozzolanic one leading to an additional decrease in strength along with the increase of gehlenite hydrate which has a low strength contribution. The decrease of portlandite in the neat paste leads also to the increase in the strength forming hydrating materials.

The increase of metakaolin content up to 30 %; decrease the strength as portlandite decrease which is one of the main pozzolanic reactants. The required level of Portland cement (PC) replacement by MK to be sufficient in removing CH will also depend on the MK purity and the quantity of CH produced by PC hydration, which is determined by the PC composition and w/b ratio. Finally,

Table 2. Compressive strength of the various blended cement (OPC-MK) mortar pastes at different hydration ages in magnesium chloride (water/binder of 0.60 %).

| Curing time (days) | Compressive strength (kg/cm ²) | | | | | |
|--------------------|--|--------|--------|--------|--------|--------|
| | MK content (%) | | | | | |
| | 0 | 10 | 15 | 20 | 25 | 30 |
| 0 | 106.4 | 114.4 | 116.7 | 118.9 | 120.1 | 99.4 |
| 1 | 111.7 | 129.63 | 148.2 | 161.6 | 165.7 | 133.3 |
| 3 | 117.4 | 130.95 | 152.54 | 164.9 | 173.1 | 142.9 |
| 7 | 118.55 | 132.33 | 167.75 | 174.66 | 177.94 | 156.4 |
| 90 | 121.84 | 139.22 | 179.65 | 184.89 | 200.68 | 172.9 |
| 180 | 125.66 | 141.01 | 188.78 | 194.66 | 219.7 | 184.02 |
| 270 | 131.3 | 152.77 | 200.01 | 203.5 | 228.3 | 209.13 |
| 360 | 137.45 | 155.73 | 205.62 | 210.1 | 235.94 | 217.52 |

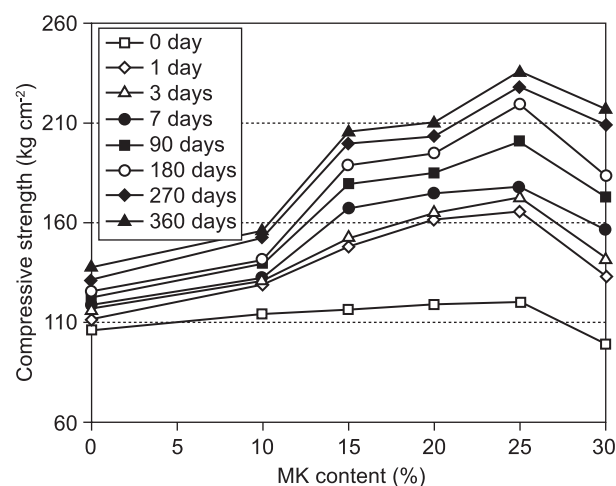


Figure 9. Compressive strength of the various blended cement (OPC-Mk) mortar pastes at different hydration ages in magnesium chloride (water/binder of 0.60 %).

the strengths of blended cement specimens containing 30 % MK are lower than containing 25 wt.% MK ones, but they are higher than that the neat OPC mortar due to the effectiveness of the pozzolanic reaction.

The conclusions elucidated from SEM emphasize the data from XRD and DTA, where the CSH increase with time (Figure 7). Where the microstructure exhibit a pronounced increase in ill-crystalline CSH with time, whereas the FS that formed at later ages (90 day) that spread all over the surface so that strengthen the structure. Also, the brucite that formed as a by product from the reaction of magnesium chloride and free lime able to encapsulate the hydration products protecting them against further deterioration. But at later age of 360 days, exhibit a different performance where the EDX analysis interpret the inclusion of chloride ions within hydration materials preventing them from further formation of FS and improving the microstructure and chloride binding behavior [23].

At 25 % MK, the CSH (I) fill the pores with the presence of crystalline CSH leading to higher compressive strength. The sharp reduction in the strength values is apparent at 30% MK content of OPC-MK blend is related to the detection of unreacted MK grains in the SEM micrographs [13, 24], as well as the presence of excess amount of gehlenite hydrate instead of FS that has lower binding properties. In spite of the strength decrease at 30 % MK, it not proportional to the neat mortar due to the effective of pozzolanic reaction of MK and free lime forming additional CSH.

Bulk Density

The bulk density and water absorption of blended cement mortar containing variable Mk contents that immersed in magnesium chloride up to 360 days are shown in Table 3 and Figure 10. The results illustrate increase of bulk density with curing time, overcoming that of the reference mixes, indicating the progress of hydration as well as formation and accumulation of CSH phases. The bulk density has the same trend as compressive strength i.e., increasing up to 25 % MK and then decreases at 30 % MK.

The increase of bulk density up to 25 % MK is due to the increase of binding materials as well as the increase of particle compaction resulting from the very fine pore structure (<0.3 μm) of MK which lead to more compaction and densifying of the mortar structure. The decrease in bulk density at 30 % MK is due to the cessation of the pozzolanic reaction effect of MK on cement component of blended cement mortars which results in an increase in total porosity and then decrease the bulk density.

Finally, it can be seen that at up to 30 % replacement, MK acts as an accelerating agent, the pore size distribution is displaced toward small values, the CH content is considerably reduced, and compressive strengths are

not affected. The ability of MK to quickly consume CH was used to develop new cement matrices that allowed their reinforcement by E-glass fibers, usually destroyed in OPC [25]. The bulk density increases and the water absorption decreases in the reverse trend. Where the decrease of free lime with MK and increase of CSH lead to lowering in the water absorption up to 25 %, while the increase in MK forms excess gehlenite hydrate that has higher water content leading to an increase of water absorption.

Table 3. Bulk density of the water cured specimens for the different curing periods vs. metakaolin added (water/binder of 0.60).

| Curing time (days) | Bulk density (g/cm ³) | | | | | |
|--------------------|-----------------------------------|-------|-------|-------|-------|-------|
| | Mk content (%) | | | | | |
| | 0 | 10 | 15 | 20 | 25 | 30 |
| 0 | 1.447 | 1.450 | 1.455 | 1.466 | 1.471 | 1.440 |
| 1 | 1.451 | 1.459 | 1.483 | 1.488 | 1.494 | 1.493 |
| 3 | 1.458 | 1.493 | 1.499 | 1.501 | 1.508 | 1.498 |
| 7 | 1.484 | 1.494 | 1.505 | 1.514 | 1.523 | 1.499 |
| 90 | 1.535 | 1.561 | 1.565 | 1.572 | 1.589 | 1.555 |
| 180 | 1.587 | 1.590 | 1.610 | 1.622 | 1.633 | 1.574 |
| 270 | 1.750 | 1.890 | 1.920 | 1.930 | 1.940 | 1.870 |
| 360 | 1.800 | 1.910 | 1.937 | 1.942 | 1.955 | 1.890 |

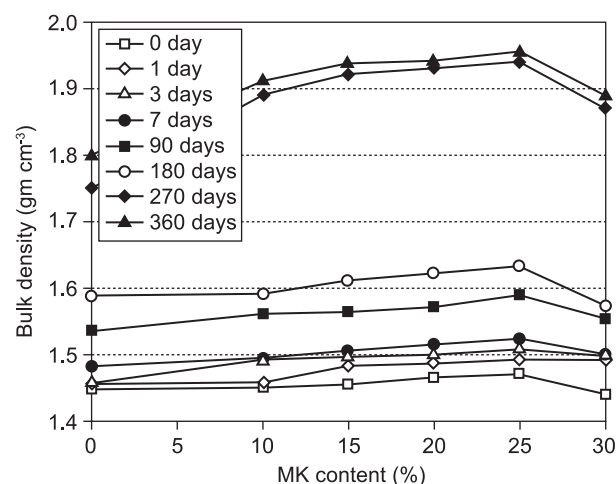


Figure 10. Bulk density of the various blended cement (OPC-MK) mortar pastes at different hydration ages in magnesium chloride (water/binder of 0.60 %).

CONCLUSIONS

1. Metakaolin provide a good resistance to aggressive chloride solution by consuming liberated lime and so prevent the formation of Friedel's salt.
2. The maximum development of compressive strength was achieved for the specimens made from OPC-MK blended cement mortars containing a metakaolin content of 25 wt.%.

3. Microstructure of the MK-blended mortar exhibit a homogeneous and a compact structure, where the optimum mix of 25 wt.% MK provide a pronounced development in the hydration materials as well as a relatively low porosity leading to an enhancement in the mechanical properties.
4. Bulk densities of all MK mortar specimens are between 1.4-2 gm/cm³ according to the Egyptian Standards Specifications 1292(1992), increases with MK up to 25 % and decreases up to 30 %.

References

1. Janotka I., Puertas F., Palacios M., Kuliffayová M., Varga C.: *Construction and Building Materials* 24, 791 (2010).
2. Cachim P., Velosa A.L., Rocha F.: *Construction and Building Materials* 24, 71 (2010).
3. Badogiannis E., Tsivilis S.: *Cement and Concrete Composites* 31,128 (2009).
4. Siddique R., Klaus J.: *Applied Clay Science* 43, 392 (2009).
5. Kim H.S., Lee S.H., Moon H.Y.: *Construction and Building Materials* 21, 1229 (2007).
6. Asbridge A.H., Page C.L., Page M.M.: *Cem. Concr. Res.* 32, 1365 (2002).
7. Asbridge A.H., Chadbourn G.A., Page C.L.: *Cem. Concr. Res.* 31, 1567 (2001).
8. Gruber K.A., Ramlochan T., Boddy A., Hooton R.D., Thomas M.D.A.: *Cem. Concr. Compos.* 23, 479 (2001).
9. Boddy A., Hooton R.D., Gruber K.A.: *Cem. Concr. Res.* 31, 759 (2001).
10. Khatib J.M., Wild S.: *Cem. Concr. Res.* 26, 1545 (1996).
11. Saikia N., Kato S., Kojima T.: *Thermochimica Acta* 44, 16 (2006).
12. Kakali G., Perraki T., Tsivilis S., Badogiannis E.: *Applied Clay Science* 20, 73 (2001).
13. Ambroise J., Murat M., Pera J.: *Cement Concrete Research* 15, 261 (1985).
14. Taha A.S., El-Didamony H., Abo EL-enein S.A., Amer H.A.: *Zement-Kalk-Gips* 34, 351 (1981).
15. ASTM C109M-07, "Standard Test Method for Compressive Strength of Hydraulic Cement Mortars", (2007).
16. Ramachandran V.S.: *Applications of Differential Thermal Analysis in Cement Chemistry*, pp. 55 – 80, Chemical Publishing Company, Inc., New York 1969.
17. Egyptian Standards, "Concrete Building Units Used in Non Load and Load Bearing Walls", Egyptian Organization for Standardization, Cairo, Egyptian Standards 1292 (1992).
18. Ambroise J., Maximilien S., Pera J.: *Advanced Cement Based Materials* 1, 161 (1994).
19. Kostuch J.A., Walters G.V., Jones T.R.: "High Performance Concretes Incorporating Metakaolin: A Review", R.K. Dhir, M. Roderick Jones (Eds.), *Concrete 2000 II, Economic and Durable Construction through Excellence*, Dundee University, 2, 1799-1811(1993).
20. Cohen M.D., Bentur A.: *ACI Mater J.* 85, 148 (1988).
21. Wild S., Khatib J.M., Jones A.: *Cement and Concrete Research* 26, 1537 (1996).
22. Crennan J.M., Dyczek J.R.L., Taylor H.F.W.: *Cement and Concrete Research* 2, 277 (1972).
23. Dhir R.K., Jones M.R.: *Fuel* 78, 137 (1999).
24. Klimesch D.S., Ray A.: *Thermochimica Acta* 307, 167 (1997).
25. Perá J., Dejean J., Ambroise J.: *Proceedings of the International Symposium "Composite Materials with Textile Reinforcement for Use in Building Construction"*, Hamelin P., Verchery G., Eds., pp. 191-202, Lyon, France 1990.